

Photoemission study of the upper limit to the change of the local exchange splitting at finite temperature

R. J. H. Kappert, H. R. Borsje, and J. F. van Acker

Research Institute for Materials, University of Nijmegen, Toernooiveld, NL-6525 ED Nijmegen, The Netherlands

K. Horn and H. Haak

Fritz-Haber-Institut der Max-Planck-Gesellschaft zur Förderung der Wissenschaften, Faradayweg 4-6, D-1000 Berlin 33, Federal Republic of Germany

K. H. J. Buschow

Philips Research Laboratories, NL-5600 JA Eindhoven, The Netherlands

J. C. Fuggle

Research Institute for Materials, University of Nijmegen, Toernooiveld, NL-6525 ED Nijmegen, The Netherlands

(Received 6 July 1990)

A photoemission study at both room temperature and at 80 K of the valence bands of the disordered alloys *PdFe*, *PdNi*, *PdCo*, and *PtFe* is presented. The Cooper-minimum effect is used to study the impurity contribution to the photoemission signal, and hence the local density of states at the impurity site. The observed differences in the photoemission signal are discussed in terms of the local exchange splitting and an attempt is presented to quantify the change in the local exchange splitting by comparison to spectra calculated with an impurity model.

INTRODUCTION

It will be the purpose of this paper to present photoemission data on the temperature dependence of local magnetic moments and exchange splittings. The exchange splitting is a parameter in Stoner's itinerant-electron band picture, which was developed more than 50 years ago for metallic ferromagnets.¹ Due to its success in describing the ground-state properties, and, in particular, nonintegral magnetic moments, it still remains the basis for our present understanding of 3*d*-transition-metal ferromagnetism at low temperatures.

Nevertheless, there are problems with the Stoner model and its use to compute finite-temperature properties. We note that, in the Stoner model, the local moment reduces proportionally with the spontaneous magnetization when approaching the critical temperature T_c . However, the T_c calculated by the Stoner theory (the Stoner temperature) is 5–10 times higher than experimental values (see, e.g., Ref. 2). Moreover, the near-perfect Curie-Weiss behavior of the magnetic susceptibility found in nearly all itinerant magnetic systems cannot be predicted by Stoner theory.³ Also, there is evidence from neutron scattering^{4,5} (since contested^{6,7}) that seemed to indicate the existence of spin waves, and therefore of magnetic moments, above T_c .

A fundamental reason for Stoner theory to fail at higher temperatures is the neglect of low-energy collective modes as elementary excitations. A number of models specifically incorporate these modes. Limiting cases are the "local band theory" (LBT),^{8–11} assuming strong short-range magnetic order on a range of 20 Å above T_c ,

and the "disordered-local-moment" (DLM) theory,^{12–14} that assumes no short-range order. Both theories assume transverse fluctuations of the magnetic moment (e.g., spin waves). Moriya has also tried to take into account longitudinal fluctuations.³ However, the controversy about the amount of short-range magnetic order, which for Ni is reported to be linked to the local moment,¹⁵ has persisted despite much experimental^{16–21} and theoretical^{15,22–26} work.

Persistence of a moment and local magnetic order above T_c would also be associated with exchange splitting of the bands of electronic states which may be observed more or less directly by (spin-polarized) photoemission^{27–30} and inverse photoemission.^{21,31–33} Most of the experimental work in this area has, until now, focused on the direct resolution of the \mathbf{k} -dependent exchange splitting in single crystal Fe and Ni. At low temperature these experiments actually show the spin-split electronic states, especially when the photoelectron spin is resolved explicitly (see, e.g., Ref. 33). Such experiments can give information on the variation of the exchange splitting through \mathbf{k} space. However, the interpretation of the results obtained at elevated temperatures is complicated by phonon-assisted transitions which ensure that a larger part of the Brillouin zone will be sampled at higher temperatures.

In view of the difficulties of (spin and \mathbf{k} -resolved) work with single crystals and the paucity of data, we have tried to open up a new experimental approach to the problem. We have studied random alloy systems—where crystal momentum and \mathbf{k} -conservation do not have the same relevance—of magnetic 3*d*-transition-metal (TM) impuri-

TABLE I. Critical temperatures T_c (taken from Ref. 38) and reduced temperatures $\tau = T/T_c$ for all measured alloys. The relative contribution of the impurity to the photoemission signal in the Cooper minimum is given in column 4 and is calculated from the cross sections given in Ref. 39.

		T_c (K)	τ (80 K)	τ (300 K)	Impurity contribution
<i>PdNi</i>	(5 at. %)	80	~ 1	3.8	0.45
<i>PdNi</i>	(10 at. %)	150	0.53	2.0	0.63
<i>PdCo</i>	(4 at. %)	170	0.47	1.8	0.35
<i>PdFe</i>	(10 at. %)	225	0.36	1.3	0.53
<i>PtFe</i>	(10 at. %)	170	0.47	1.8	0.50

ties in Pd and Pt. These systems are itinerant electron magnets, as can be judged by studying the Rhodes-Wohlfahrt plot (see Ref. 3, p. 131), and the critical temperatures for these systems are given in Table I. We have used angle-integrated photoemission at the Cooper minimum in the Pd *4d* or Pt *5d* cross section in order to isolate the electronic-structure effects at the magnetic impurity site.^{34,35} (This was, of course, unnecessary for the same impurities in Ag, where host and impurity *d* states do not overlap.³⁶) Finally, we have made measurements at liquid-nitrogen temperatures and at room temperature in order to compare the electronic structure of the impurity above and below T_c . The results will show that the changes are very small indeed. In order to try to give some semiquantitative measure of the size of the upper limit of the changes in the exchange parameter consistent with these small changes, we then proceed to analyze the data with the generalized Clogston-Wolff model described earlier.³⁷

EXPERIMENT

The polycrystalline alloys *PdCo*(4 at. %), *PdNi*(5 and 10 at. %), *PdFe*(10 at. %), and *PtFe*(10 at. %) were prepared by arc melting. X-ray diffraction was used to check that the samples were single phase. All samples were found to be ferromagnetic (see Table I) at liquid-nitrogen temperatures and to be paramagnetic at room temperature, with the exception of *PdNi*(5 at. %), which was found to be paramagnetic at both temperatures.

Samples were mounted on a copper block attached to a cryostat. The cryostat consisted of a hollow tube mounted on a rotatable manipulator. Low temperatures were obtained by filling the cryostat with liquid nitrogen. Temperatures were monitored by a chromel-alumel thermocouple attached to the sample block.

The photoemission experiments were carried out at the HE-TGM2 beamline at BESSY (Berliner Elektronenspeicherring-Gesellschaft für Synchrotronstrahlung). All experiments were performed at 130 eV photon energy with a resolution of typically 0.6 eV. The spectra were taken at normal incidence, collecting electrons with a takeoff angle up to $\sim 40^\circ$ with respect to the surface normal.

The samples were cleaned by scraping *in situ* before each measurement. The base pressure was about 1×10^{-10} mbar, and dropped to about 5×10^{-11} mbar with the cryostat at 80 K. For low-temperature measurements, samples were scraped after cooling down. Pro-

longed measurements were done in several sessions with repeated scraping before each run.

After each run the spectrum was carefully checked for reproducibility. Enough spectra were taken to ensure that the peak intensity in the summed spectrum would be of the order of 100 000 counts.

Absolute normalization of the spectra was not possible. For each sample, we normalized the spectra to the integrated intensity of the valence band, after subtracting a background representing inelastic loss of the photoelectrons, so that, at a chosen point below the valence band, the intensity vanished.

RESULTS AND INTERPRETATION

The valence-band photoemission spectra of the disordered alloys *PdNi*(5 and 10 at. %), *PdCo*(4 at. %), *PdFe*(10 at. %), and *PtFe*(10 at. %) are presented in Fig. 1. The dotted curves were recorded at liquid-nitrogen temperature (~ 80 K). Room-temperature curves are shown as solid lines where they differed significantly from the low-temperature spectra.

In connection with the general features of the spectra, we note that, in general, the states at the bottom of the valence band in these materials contribute proportionally less to the spectra because the single-particle photoemission matrix elements are lower⁴⁰ and because the high-binding-energy regions contribute proportionally more to the satellite regions.^{41–43} The width of the single-particle region of the spectrum is ~ 6 eV, which corresponds to the width of the Pd or Pt hosts bands. About $\sim 50\%$ of the spectrum in this region is from the host and its shape is expected to be similar to that of pure Pd or Pt. The other $\sim 50\%$ comes from the impurity (Table I). The shape of this contribution also reflects many features of the host because there is strong hybridization between impurity and host states.^{35,44} However, this contribution also reflects the effective atomic energy levels of the impurities, and hence, the exchange splitting of spin-up and spin-down levels.^{35,44}

Below the single-particle region (and partly overlapping it) we see a large signal due primarily to inelastically scattered electrons. This region also contains the contributions from satellites and many-body excitations.^{41–43} In general, this region shows little structure. Exceptions are the weak features at ~ 8 and ~ 11 eV in the *PdNi* alloy spectra. These could be confused with peaks from a very low level of CO contamination (see, e.g., Ref. 45). We found the intensity of these peaks to be remarkably

constant from run to run and not to increase significantly with exposure to the vacuum. We are thus inclined to attribute them to many-body satellites intrinsic to the *PdNi* system and not to CO. However, because they are so constant, their presence is not relevant to the central theme of this paper.

For all systems, the difference between room-

temperature and 80 K spectra is presented, magnified five times. It can be observed that the differences between room-temperature and 80 K spectra are small, especially in the high-binding-energy region. Most changes in the photoemission signal are found at the Fermi level. Of the various spectra, only *PdCo* and *PtFe* do not show any significant structure in the difference spectra.

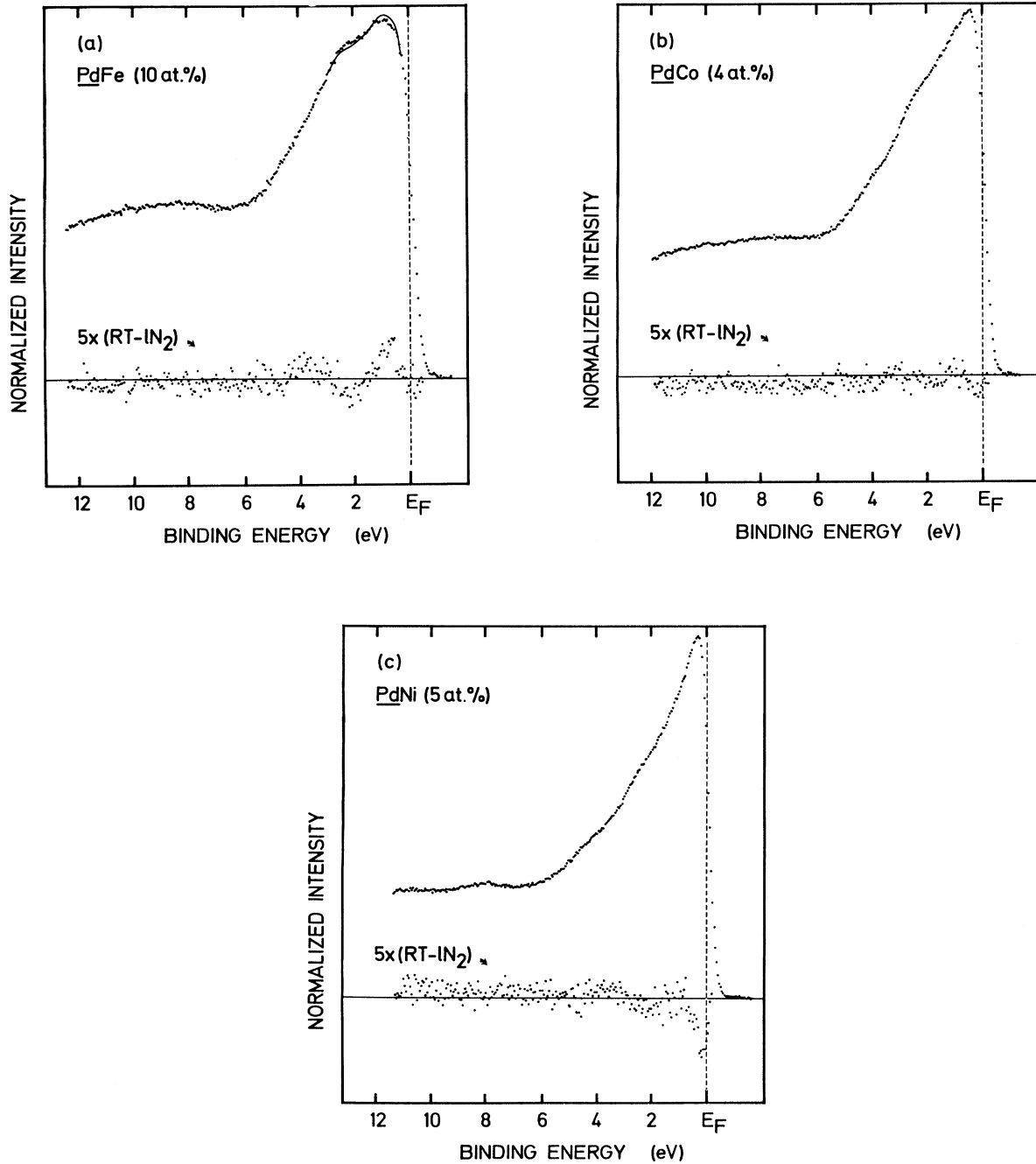


FIG. 1. Valence-band photoemission spectra *PdFe*, *PdCo*, *PdNi*(5 and 10 at. %), and *PtFe*, taken at 130 eV photon energy. The upper dotted curves represent the spectra taken at liquid-nitrogen temperatures. Solid lines represent the room-temperature spectra if they substantially differ from the liquid-nitrogen temperature spectra. The difference between these spectra, magnified five times, is presented by the lower dotted curve.

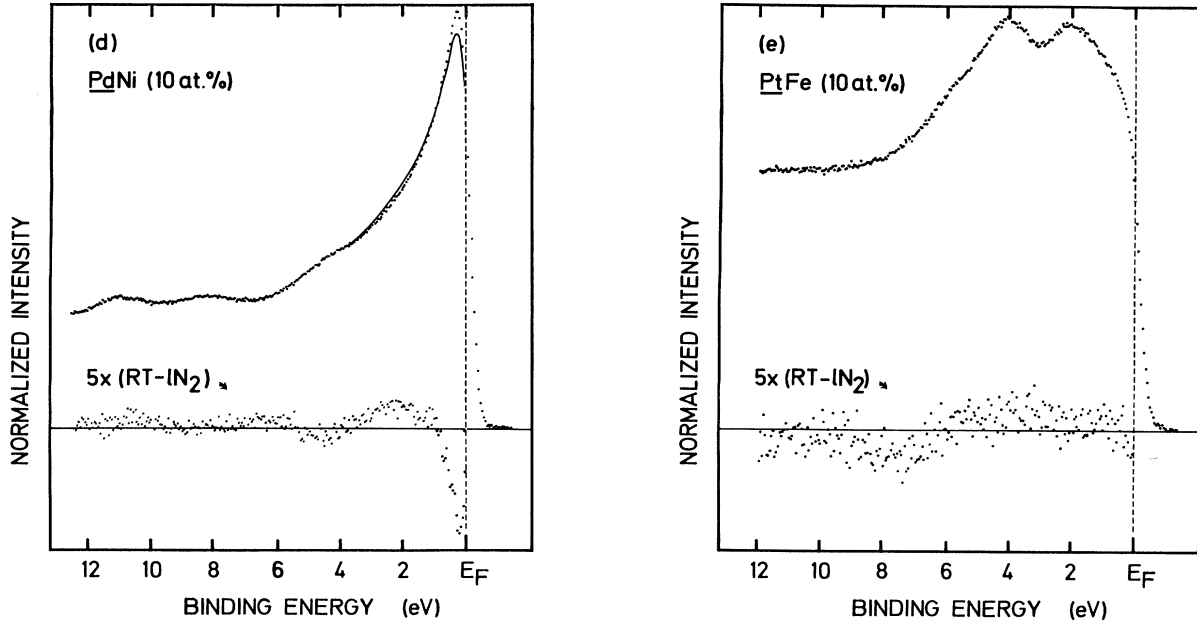


FIG. 1. (Continued).

We will discuss in detail below the nature and origin of the small differences found in these spectra. First, however, we stress how small the differences are. This is extremely relevant because in all cases the contribution of the impurity $3d$ states to these spectra is of the order of $\sim 50\%$ (see Table I). Moreover, in the dilute limit of Pd- or Pt-based alloys, we expect a strong redistribution of the local density of states (DOS) with small changes in the local magnetic moment or the effective exchange parameter as will be discussed below. Thus, a large change of the local moment would have been immediately noticeable and it must be concluded that the TM moments persist almost unchanged above T_c .

The most pronounced differences were found in the PdNi(10 at.%) spectrum. The spectrum at room temperature exhibits less intensity at the Fermi level than the 80 K spectrum. A little more spectral weight is found around ~ 2 eV below E_F as compared to the low-temperature spectrum. The PdNi(5 at.%) difference spectrum resembles that of the 10 at. % Ni in Pd, but the structure at the Fermi level is reduced by a factor of ~ 2 , corresponding to the different amounts of Ni in the alloys.

The differences observed in the PdFe spectra are opposite to those of PdNi(10 at. %). Here the intensity of the room-temperature spectrum near the Fermi level is higher than the 80 K spectrum, while at higher binding energy (~ 2 eV) the intensity is lower. These changes are very weak and similar to those caused by exposure to gases for periods longer than 1 h. It is therefore possible that the differences observed are associated with contamination of the sample, despite the severe precautions taken.

DISCUSSION

Magnetic impurities in Pd (Pt) can be described by a majority-spin state and a minority-spin state, separated in

energy by the exchange interaction. These states will hybridize with the host d band. We can see from the calculated DOS for Fe impurities in Pd (Refs. 46 and 47) that the minority-spin states are pushed above the Fermi level by the hybridization with the Pd d -band because the effective energy level of the Fe minority-spin states is situated above the Pd d -band centroid. The calculations show Fe majority-spin states to be situated in the host d band, the largest weight of the majority-spin states being at 2–5-eV binding energy.

For Ni in Pd (Pt),^{46,47} the situation is slightly different. The calculated DOS for Ni in Pd shows that most of the minority-spin states are situated at the top of the valence band. The Ni majority-spin states are calculated to have their largest weight at 0–2-eV binding energy. For Co, the theoretical results are intermediate between Fe and Ni.^{46,47} The large photoemission intensity at the Fermi level for Ni and Co in Pd is thus mainly due to minority-spin states.

To show the sensitivity of the photoemission spectrum to the (local) magnetic structure we will present results of calculations using a generalized Clogston-Wolff (CW) model.³⁷ In this model the impurity is represented by the energy difference Δ between the host d -band centroid and the impurity state and a renormalization of the impurity-host hybridization potential. The results of the CW calculation with Δ and the hybridization as free parameters to be fitted reproduce the self-consistent Korringa-Kohn-Rostoker (KKR) results remarkably well^{46,47} and provide a suitable basis for data interpretation.

For Fe in Pd, the impurity-host interaction reduced to 75% of the Pd-Pd hybridization yields the best results.⁴⁴ The effective impurity levels are found at $\Delta = -1.06$ eV for the majority-spin level, and $\Delta = 1.99$ eV for the minority-spin level.⁴⁴ The resulting local density of states (LDOS) for majority-spin states (solid line) and

minority-spin states is shown in the bottom panel of Fig. 2.

As mentioned in the general survey above, we observe the Fe majority-spin states to be separated from the minority-spin states due to the exchange interaction. The impurity-host hybridization has resulted in the Fe majority-spin LDOS reflecting the shape of the Pd host d band, while the minority-spin states have been pushed above the Fermi level.

Reducing the magnetic moment at the Fe site by 1%, while keeping the local number of d electrons constant, we obtain the LDOS shown in the middle panel of Fig. 2. (This yields results similar to reducing the local exchange splitting by $\sim 5\%$.) Although the minority-spin state LDOS hardly changes, significant changes can be seen to occur in the majority-spin part of the LDOS as the weight of the majority-spin band is shifting towards the Fermi level. We may already conclude from a comparison of Figs. 2(a) and 2(b) with the experimental results that there is only weak temperature dependence of the magnetic moment at the Fe site, and of the local ex-

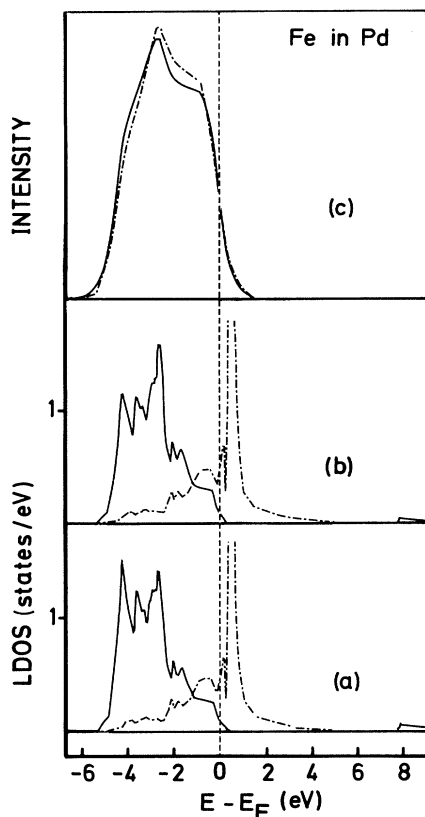


FIG. 2. Fe impurity in Pd. (a) LDOS on the Fe site obtained from the Clogston-Wolff (CW) model calculations. (b) LDOS on the Fe site obtained from the CW calculations with the local magnetic moment reduced to 99% of the value of (a). (c) The occupied part of the LDOS on Fe broadened to simulate instrument (Gaussian, FWHM 0.6 eV) and lifetime (Lorentzian, FWHM 0.1 ($E - E_F$) eV) effects. Single-electron matrix elements (see Ref. 40) are taken into account by multiplying a sloping line of 15%/eV. Solid curve: broadened DOS obtained from (a). Dash-dotted curve: broadened DOS obtained from (b).

change splitting. However, we must try to simulate spurious effects, such as instrumental and lifetime broadening, binding-energy dependence of the photoemission matrix elements (ME), and inelastic losses to further quantify this statement. To this end we have broadened the occupied part of the LDOS from Figs. 2(a) and 2(b) to simulate instrumental and lifetime broadenings, and multiplied the LDOS by a sloping line to simulate ME effects (see the figure caption). We are aware of the limitations of this procedure, but it does show that, even after taking into account spurious effects (plus the fact that $\sim 50\%$ of the photoemission signal still comes from Pd), large changes in local exchange splitting at the Fe site would still be recognizable. We must conclude that the changes in local moment at the Fe site in Pd are less than $\sim 1\%$ (corresponding to changes in the local exchange splitting smaller than $\sim 5\%$) over the temperature range studied.

Similar conclusions can be drawn for Co in Pd and Fe in Pt. For Ni in Pd the situation is different. Ni is expected to be the least sensitive to changes in the local moment, as can be seen in Fig. 3, because the exchange splitting is so low. The local moment on Ni in mean-field theory (see, e.g., Ref. 13) is expected to decrease $\sim 30\%$ over the temperature range of the experiment, whereas the Fe local moment is expected to decrease only $\sim 5\%$. We observed the largest changes for the PdNi system, but they were different to those calculated. If the differences observed are of magnetic nature, we would expect an increase of the DOS at E_F going to higher temperatures, whereas we observe a decrease. Thus, the effects observed in the PdNi systems are a puzzle to us, but here too the main conclusion is that temperature-induced changes in the effective atomic moment and the exchange splitting are small.

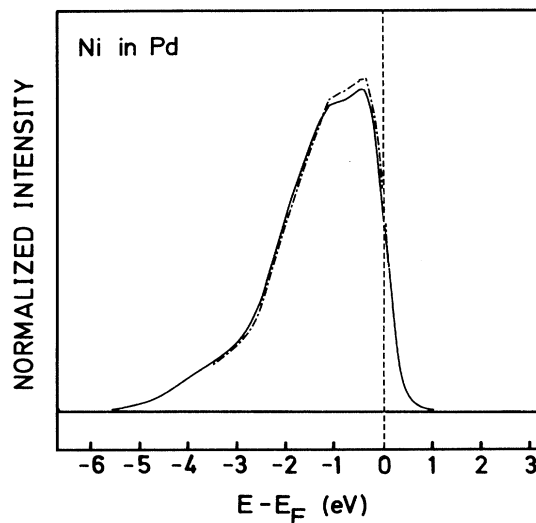


FIG. 3. Solid curve: CW calculations for Ni impurity in Pd. LDOS on Ni site broadened as in Fig. 2(a). Dash-dotted curve: as for the solid curve, but calculated with the local magnetic moment reduced to 98%.

CONCLUDING REMARKS

In this paper we have reported a study of the temperature dependence of the photoemission spectra of Pd and Pt with magnetic impurities. The spectra were taken at the Pd-Pt Cooper minima so that typically $\sim 50\%$ of the signal came from the impurity, because the aim of the research was to study the change in local exchange splitting at the impurity site. The temperature dependence of the spectra was very weak. Comparison with model calculations indicate that the changes observed are not consistent with changes larger than $\sim 5\%$ in the local ex-

change splitting. Thus, our results are certainly incompatible with the collapse of the local magnetic moment on the impurity site at T_c when the long-range magnetic order collapses in these materials.

ACKNOWLEDGMENTS

This work has been supported in part by the Stichting voor Fundamenteel Onderzoek der Materie (FOM) with financial support from the Nederlandse Stichting voor Wetenschappelijk Onderzoek (NWO), The Netherlands.

-
- ¹E. C. Stoner, Proc. R. Soc. London Ser. A **154**, 656 (1936).
²O. Gunnarson, J. Phys. F **6**, 587 (1976).
³T. Moriya, *Spin Fluctuations in Itinerant Magnetism*, Vol. 56 of *Solid-State Sciences* (Springer-Verlag, Berlin, 1985).
⁴H. A. Mook, J. W. Lynn, and R. M. Nicklow, Phys. Rev. Lett. **30**, 556 (1973).
⁵J. W. Lynn, Phys. Rev. B **11**, 2624 (1975).
⁶G. Shirane, Y. J. Uemura, O. Steinvoll, and J. Wicksted, J. Appl. Phys. **55**, 1887 (1984).
⁷J. Callaway, Phys. Rev. Lett. **112A**, 67 (1985).
⁸V. Korenman, J. L. Murray, and R. E. Prange, Phys. Rev. B **16**, 4032 (1977).
⁹V. Korenman, J. L. Murray, and R. E. Prange, Phys. Rev. B **16**, 4048 (1977).
¹⁰V. Korenman, J. L. Murray, and R. E. Prange, Phys. Rev. B **16**, 4058 (1977).
¹¹H. Capellmann, Z. Phys. B **34**, 29 (1979).
¹²J. Staunton, B. L. Gyroffy, A. J. Pindor, G. M. Stocks, and H. Winter, J. Magn. Magn. Mater. **45**, 15 (1984).
¹³A. J. Pindor, J. Staunton, G. M. Stocks, and H. Winter, J. Phys. F **13**, 979 (1983).
¹⁴H. Hasegawa, J. Phys. Soc. Jpn. **46**, 1504 (1979).
¹⁵E. M. Haines, Solid State Commun. **69**, 561 (1989).
¹⁶C. S. Fadley, in *Electron Spectroscopy*, edited by D. A. Shirley (North-Holland, Amsterdam, 1972), p. 781.
¹⁷R. E. Kirby, E. Kisker, F. K. King, and E. L. Garwin, Solid State Commun. **56**, 425 (1985).
¹⁸R. Clauberg, E. Haines, and R. Feder, J. Magn. Magn. Mater. **54-57**, 622 (1986).
¹⁹C. Rau and H. Kuffner, J. Magn. Magn. Mater. **54-57**, 767 (1986).
²⁰J. F. van Acker, Z. M. Stadnik, J. C. Fuggle, H. J. Hoekstra, K. H. J. Buschow, and G. Stroink, Phys. Rev. B **37**, 6827 (1988).
²¹M. Donath, Appl. Phys. A **49**, 351 (1989), and references therein.
²²H. Capellmann and V. Vieira, Solid State Commun. **43**, 747 (1982).
²³D. M. Edwards, J. Magn. Magn. Mater. **36**, 213 (1983).
²⁴R. Clauberg, E. Haines, and R. Feder, Z. Phys. B **62**, 31 (1985).
²⁵H. Hasegawa and F. Herman, J. Phys. (Paris) **49**, 1677 (1988).
²⁶W. Nolting, W. Borgiet, V. Dose, and Th. Fauster, Phys. Rev. B **40**, 5015 (1989).
²⁷D. E. Eastman, F. J. Himpsel, and J. A. Knapp, Phys. Rev. Lett. **40**, 1514 (1978).
²⁸H. Hopster, R. Raue, G. Güntherodt, E. Kisker, R. Clauberg, and M. Campagna, Phys. Rev. Lett. **51**, 829 (1983).
²⁹E. Kisker, K. Schröder, W. Gudat, and M. Campagna, Phys. Rev. B **31**, 329 (1985).
³⁰K.-P. Kämper, W. Schmidt, and G. Güntherodt, J. Phys. (Paris) **49**, 39 (1988).
³¹J. Unguris, A. Seiler, R. J. Celotta, D. T. Pierce, P. D. Johnson, and N. V. Smith, Phys. Rev. Lett. **49**, 1047 (1982).
³²H. Scheidt, M. Glöbl, V. Dose, and J. Kirschner, Phys. Rev. Lett. **51**, 1688 (1983).
³³D. T. Pierce, Surf. Sci. **189**, 710 (1987), and references therein.
³⁴J. W. Cooper, Phys. Rev. **128**, 681 (1962).
³⁵J. F. van Acker, P. W. J. Weijs, J. C. Fuggle, K. Horn, W. Wilke, H. Haak, H. Saalfeld, H. Kühlenbeck, W. Braun, G. P. Williams, D. Wesner, M. Strongin, S. Krummacker, and K. H. J. Buschow, Phys. Rev. B **38**, 10463 (1988).
³⁶D. van der Marel, C. Westra, G. A. Sawatzky, and F. U. Hillebrecht, Phys. Rev. B **31**, 1936 (1985).
³⁷W. Speier, J. F. van Acker, and R. Zeller, Phys. Rev. B **41**, 2753 (1990); see also, Ref. 36.
³⁸J. A. Mydosh and G. J. Nieuwenhuys, in *Ferromagnetic Materials*, edited by E. P. Wohlfahrt (North-Holland, Amsterdam, 1980), Vol. 1, Chap. 2.
³⁹J. J. Yeh and L. Lindau, At. Data Nucl. Data Tables **32**, 1 (1985).
⁴⁰W. Speier, J. C. Fuggle, P. Durham, R. Zeller, R. J. Blake, and P. Sterne, J. Phys. C **21**, 2621 (1988), and references therein.
⁴¹A. Liebsch, Phys. Rev. Lett. **43**, 1431 (1979).
⁴²A. Liebsch, Phys. Rev. B **23**, 5203 (1981).
⁴³J. C. Fuggle, F. U. Hillebrecht, R. Zeller, Z. Zolnieriek, P. A. Bennet, and Ch. Freiburg, Phys. Rev. B **27**, 2145 (1982), and references therein.
⁴⁴J. F. van Acker, Ph.D. thesis, University of Nijmegen, 1990.
⁴⁵D. E. Eastman and J. K. Cashion, Phys. Rev. Lett. **27**, 1520 (1971).
⁴⁶A. Oswald, Ph.D. thesis, Kernforschungsanlage Jülich, 1985.
⁴⁷A. Oswald, R. Zeller, and P. H. Dederichs, Phys. Rev. Lett. **56**, 1419 (1986).